

Solid-State $^{47,49}\text{Ti}$ NMR Determination of the Phase Distribution of Titania Nanoparticles

C. Gervais,[†] M. E. Smith,^{*,†} A. Pottier,[‡] J.-P. Jolivet,[‡] and F. Babonneau[‡]

Department of Physics, University of Warwick, Coventry, CV4 7AL, United Kingdom, and
Chimie de la Matière Condensée, Université Pierre et Marie Curie, 4 Place Jussieu,
75252 Paris Cedex 05, France

Received October 9, 2000

$^{47,49}\text{Ti}$ solid-state NMR spectra are reported from TiO_2 nanoparticles. Particles heated below 700 °C are predominantly anatase. The corresponding $^{47,49}\text{Ti}$ NMR spectra can be simulated by using the NMR interaction parameters determined from bulk polycrystalline TiO_2 with an additional Lorentzian smoothing, which increases as the particle size, as determined by X-ray diffraction, decreases. Above 700 °C conversion to rutile increases with increasing calcination temperature. XRD and solid-state NMR provide complementary quantification of the phase distribution with very good agreement between the techniques when there are comparable quantities of rutile and anatase present. At low anatase content NMR is more sensitive to the phase distribution.

Introduction

The well-known technological importance of titania-based materials has resulted in applications such as pigments,¹ gas and humidity sensors^{2,3} catalysts,⁴ photocatalysts,⁵ and photovoltaics.⁶ The optical, electrical, and catalytic properties of these materials strongly depend not only on the crystalline phase present but also on the morphology and size of the particles.^{7–9}

Most solid-state NMR studies of TiO_2 -related materials have applied ^{17}O including investigation of the structure of crystalline titania,¹⁰ TiO_2 gels,^{11,12} and TiO_2 nanoparticles.¹³ ^{17}O NMR readily distinguishes the three crystalline TiO_2 polymorphs, anatase, rutile, and brookite, from their distinct isotropic chemical shifts. To allow good signal-to-noise spectra to be readily acquired, ^{17}O enrichment is necessary because of the very low natural abundance of this nucleus (0.037%).

This is straightforward and relatively inexpensive for some sol–gel routes^{11,12} but would be quite expensive for the aqueous synthesis route used in this investigation. Here, monodisperse TiO_2 nanoparticles are obtained by precipitation from TiCl_4 in an aqueous solution of HCl, the size of the particles being adjusted over the nanometer scale (5–10 nm) by controlling the acidity of the precipitation medium.¹⁴

An alternative NMR approach is to examine $^{47,49}\text{Ti}$, which has been shown to give useful information about Ti-based oxides and metals^{15,16} despite the intrinsic difficulty of observing these nuclei. To date, few solid-state Ti NMR studies have been published (see ref 17 for a recent review) because of the properties of the two magnetically active isotopes, ^{47}Ti ($I = 5/2$) and ^{49}Ti ($I = 7/2$). The isotopes both have a low natural abundance (7.28% for ^{47}Ti , 5.51% for ^{49}Ti) and small gyromagnetic ratios (γ). These factors combine to produce relatively low intrinsic detection sensitivity. However, the main experimental difficulty is that both isotopes have moderately large quadrupole moments (Q) in the ratio $^{49}\text{Q}/^{47}\text{Q} = 0.8275$. Usually, the second-order quadrupolar broadened central ($1/2, -1/2$) transition is observed with relative broadening $\Delta\nu^{47}/\Delta\nu^{49} \sim 3.437$.¹⁸ For comparison with ^{27}Al the relative broadening of ^{49}Ti is at least 5.74 greater for sites with the same structural distortion, largely through the effect of the low γ . Titanium NMR has the additional difficulty that the isotopes have almost identical γ 's, so that even at 14.1 T the resonance frequencies differ by only ~ 9 kHz. Given the typical widths of the resonances observed, most spectra will

* To whom correspondence should be addressed. E-mail: M.E.Smith.1@warwick.ac.uk.

[†] University of Warwick.

[‡] Université Pierre et Marie Curie.

(1) Balfour, J. G. *Technological Applications of Dispersions*; Marcel Dekker: New York, 1994.

(2) Yeh, Y. C.; Tseng, T. T.; Chang, D. A. *J. Am. Ceram. Soc.* **1989**, *72*, 1472.

(3) Munuera, G.; Gonzalez-Eliphe, A. R.; Munoz, A.; Fernandez, A.; Soria, J.; Conesa, J. *Sensors Actuators* **1989**, *18*, 337.

(4) Bond, G. C.; Fischer, S. F. *Appl. Catal.* **1991**, *71*, 1.

(5) Fujishima, A.; Honda, K. *Nature* **1972**, *37*, 238.

(6) O'Regan, B.; Grätzel, M. *Chem. Rev.* **1995**, *95*, 49.

(7) Bickley, R. I.; Gonzalez-Carreno, T.; Lees, J. S.; Palmisano, L.; Tilley, R. J. D. *J. Solid State Chem.* **1991**, *92*, 178.

(8) Krol, R.; Goosens, A.; Schoonman, J. *J. Electrochem. Soc.* **1997**, *144*, 1723.

(9) Moritz, T.; Reiss, J.; Diesner, K.; Su, D.; Chemseddine, A. *J. Phys. Chem. B* **1997**, *101*, 8052.

(10) Bastow, T. J.; Stuart, S. N. *Chem. Phys.* **1990**, *143*, 459.

(11) Bastow, T. J.; Moodie, A. F.; Smith, M. E.; Whitfield, H. J. *J. Mater. Chem.* **1993**, *3*, 697.

(12) Bastow, T. J.; Doran, G.; Whitfield, H. J. *Chem. Mater.* **2000**, *12*, 436.

(13) Scolan, E.; Magnenet, C.; Massiot, D.; Sanchez, C. *J. Mater. Chem.* **1999**, *9*, 2467.

(14) Pottier, A. Ph.D. Thesis, Université Pierre et Marie Curie, Paris, France, 1999.

(15) Bastow, T. J.; Gibson, M. A.; Forwood, C. T. *Solid State NMR* **1998**, *12*, 201.

(16) Padro, D.; Howes, A. P.; Smith, M. E.; Dupree, R. *Solid State NMR* **2000**, *15*, 231.

(17) Smith, M. E. *Annu. Rep. NMR Spectrosc.* **2000**, *43*, 121.

(18) Smith, M. E.; van Eck, E. R. H. *Prog. NMR Spectrosc.* **1999**, *34*, 159.

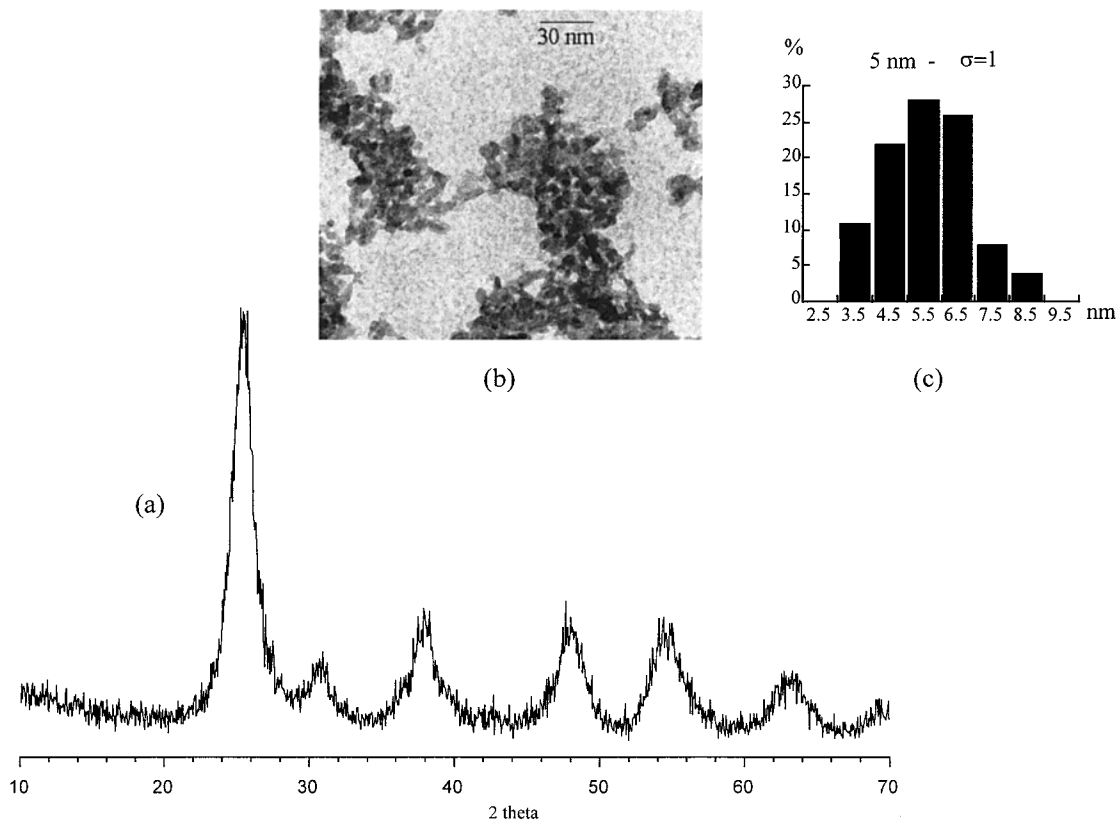


Figure 1. (a) XRD pattern, (b) TEM micrograph, and (c) particle size distribution of as-made anatase nanoparticles.

Table 1. ^{49}Ti NMR Parameters Extracted from the Simulations of the Different Bulk Polycrystalline Phases of TiO_2

sample	^{49}Ti δ_{iso} (ppm) (± 5)	$^{49}\text{C}_Q$ (MHz) (± 0.1)	η (± 0.1)
anatase	-67	4.6	0.1
rutile	-15	13.4	0.2
brookite	-165	10.0	0.55

consist of completely overlapped resonances from the two isotopes.

Despite these problems titanium NMR spectra have been reported from all three polymorphs of titania^{15,19–21} with the quadrupole coupling constant C_Q varying by a factor of ≈ 3 and the isotropic chemical shifts covering a range of ≈ 200 ppm (see Table 1 of ref 12). A TiO_2 gel annealed at different temperatures has recently been studied by $^{47,49}\text{Ti}$ NMR.²² Despite significant overlap of the resonances, there were sufficient spectral features to unambiguously identify anatase and rutile. This encourages the view that titanium solid-state NMR could have great potential for characterizing such systems.

This paper examines the influence of the size and crystallinity of TiO_2 nanoparticles on the shape of the corresponding $^{47,49}\text{Ti}$ NMR spectra. The spectra are then simulated to quantify the distribution of anatase and rutile phases in these nanoparticles and the changes that occur upon annealing at high temperatures. A careful comparison is made between the phase distribution in these particles as determined by $^{47,49}\text{Ti}$ NMR and X-ray diffraction (XRD).

Experimental Section

Nanoparticle Synthesis. Five milliliters of pure TiCl_4 (Fluka, 98%) was first diluted in a 3 M solution of hydrochloric acid and the resulting solution ($[\text{Ti}^{4+}] = 0.7$ M) was diluted in 30 mL of distilled water. The pH of the medium was then adjusted to be 2 by the addition of 3 M sodium hydroxide and maintained at this value for 30 min. A white precipitate appeared instantaneously and the solid phase was collected by centrifugation after a week of aging at 60 °C without stirring. The precipitate was washed twice with a solution of the same pH as used for the synthesis and was then dried at room temperature under a nitrogen flow. The sample was then annealed under an ambient atmosphere for ≈ 1 h, in successive steps to 850 °C.

Particle Size Characterization. XRD patterns of all samples were collected on a Phillips PW1050 powder diffractometer using $\text{Cu K}\alpha$ radiation ($\lambda = 1.544$ Å). A range of $2\theta = 10^\circ$ – 70° was scanned at a rate of $1.5^\circ \text{ min}^{-1}$. Assuming that the line broadening is essentially due to the particle size (S), an estimate for S was made from the Debye–Scherrer equation,²³ that is, $S = (0.9 \times \lambda) / (\beta \times \cos \theta)$ where λ is the wavelength of the X-ray radiation and β is the corrected full width at half-height of a diffraction peak at angle θ . Figure 1a shows the XRD pattern recorded for the as-made nanoparticles, which is characteristic of crystalline particles of TiO_2 anatase with a small quantity of brookite ($\leq 20\%$). The mean size of the titania particles was determined from the measured line widths of the (101) and (200) diffraction lines. These two peaks are superimposed with XRD reflections of brookite, but as the proportion of brookite is always small, accurate estimates of the anatase particle size can be made. The average diameter obtained is 5 ± 0.4 nm, which is consistent with the mean size observed by TEM experiments (Figure 1b,c). The transmission electron micrograph was obtained using a JEOL 100 CX microscope, and the sample was prepared by evaporating very dilute suspensions onto carbon-coated grids. The

(19) Labouriau, A.; Earl, W. L. *Chem. Phys. Lett.* **1997**, *270*, 278.

(20) Kanert, O.; Kalem, H. *J. Phys. C* **1998**, *21*, 3909.

(21) Dec, S. F.; Davis, M. F.; Maciel, G. E.; Bronnimann, C. E.; Fitzgerald, J. J.; Han, S. S. *Inorg. Chem.* **1993**, *32*, 955.

(22) Bastow, T. J.; Whitfield, H. J. *Chem. Mater.* **1999**, *11*, 3518.

(23) Scherrer, P. *Nachr. Ges. Wiss. (Göttingen)*, 1918.

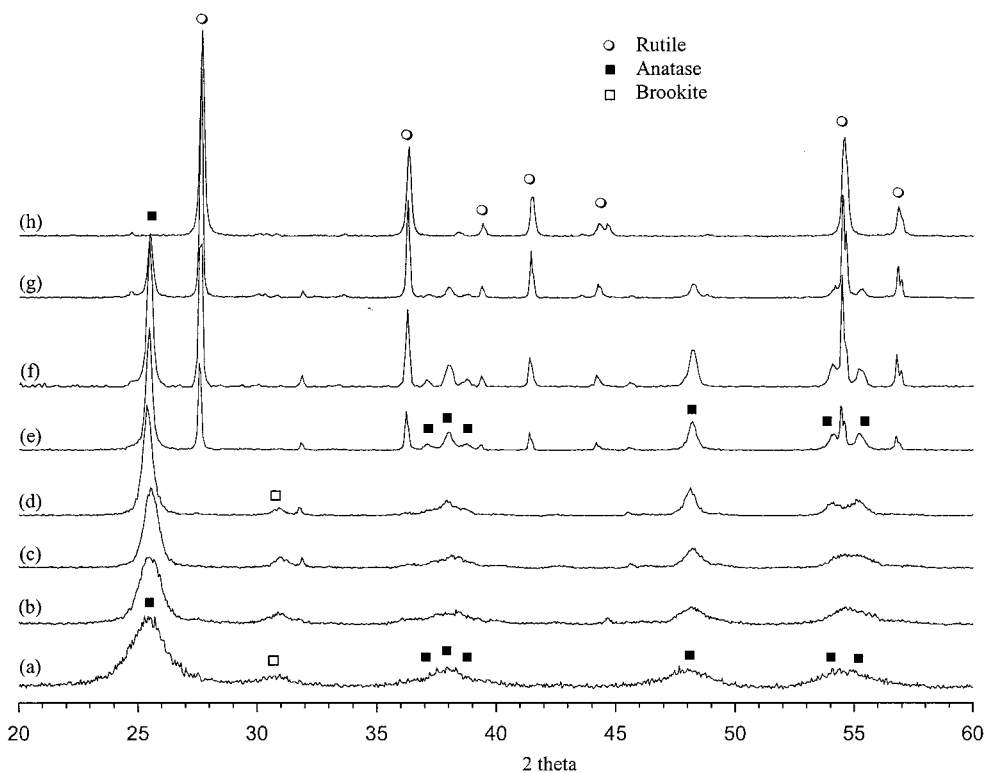


Figure 2. XRD patterns of (a) as-made TiO_2 particles and after calcination at (b) 400 °C, (c) 550 °C, (d) 650 °C, (e) 700 °C, (f) 730 °C, (g) 770 °C, and (h) 850 °C.

particle size distribution was determined by measuring the average diameter of about 100 particles.

$^{47,49}\text{Ti}$ NMR Experiments. Static NMR spectra were acquired at 33.81 MHz using a CMX Infinity 600 spectrometer with a Chemagnetics 9.5-mm MAS probe. Spectra were recorded using a spin-echo $\theta-\tau-2\theta$ pulse sequence ($\theta = 90^\circ$ corresponding to a 1.8- μs pulse length) with extended phase cycling.²⁴ τ was made sufficiently long to capture the whole echo, which was apodized by Gaussian multiplication centered at the echo maximum and Fourier transformed. As the whole echo is captured, the spectra are readily phased by zeroing the imaginary channel. A recycle delay of 1 s was employed, which was sufficiently long to ensure fully relaxed spectra, and 20 000–90 000 FIDs were typically added together. Spectra were referenced to the ^{49}Ti line of SrTiO_3 ($\delta = 0$ ppm). The observed second-order quadrupolar line shapes for the (1/2, -1/2) transition for ^{47}Ti and ^{49}Ti were fitted using a modified version of the Bruker Winfit program.²⁵

Results and Discussion

The X-ray patterns obtained for the TiO_2 particles heat-treated up to 850 °C are presented in Figure 2. Anatase and a small proportion of brookite ($\leq 20\%$) are evident below 700 °C while rutile appears at > 700 °C. As rutile is the thermodynamically stable phase, the proportion of rutile clearly increases with temperature and is the only phase observed at 850 °C. It is also evident that the peak width from anatase decreases with temperature, indicating an increase of the average particle size.

The $^{47,49}\text{Ti}$ NMR static spectra of the TiO_2 nanoparticles annealed up to 850 °C are shown in Figure 3. The line shape observed for the as-made particles resembles

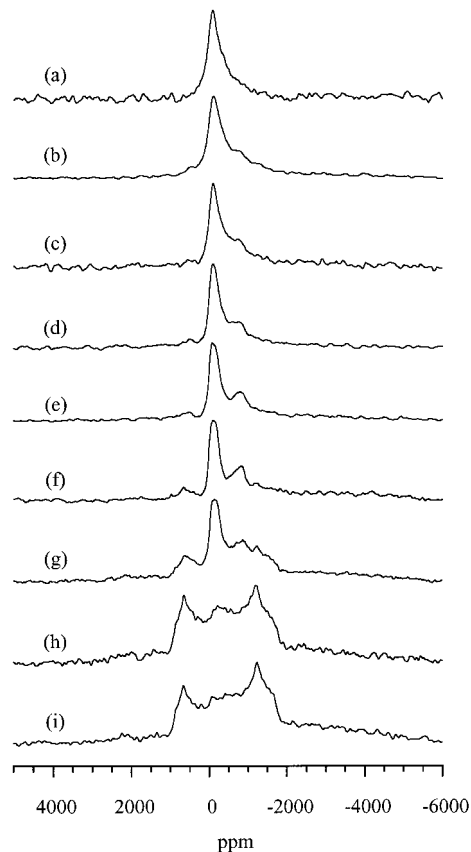


Figure 3. $^{47,49}\text{Ti}$ static NMR spectra of (a) the as-made TiO_2 particles and after calcination at (b) 400 °C, (c) 550 °C, (d) 650 °C, (e) 700 °C, (f) 730 °C, (g) 770 °C, (h) 800 °C, and (i) 850 °C.

a smeared version of an anatase spectrum (discussed below) and is quite similar to the one reported by

(24) Kunwar, A. C.; Turner, G. L.; Oldfield, E. *J. Magn. Reson.* **1986**, *69*, 124.

(25) Massiot, D.; Thiele, H.; Germanus, A. *Bruker Rep.* **1994**, *140*, 43.

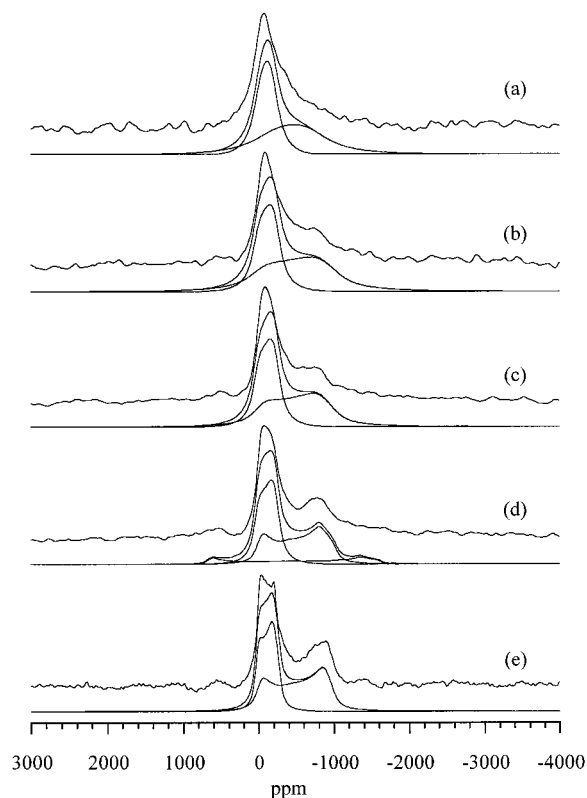


Figure 4. Experimental and simulated $^{47,49}\text{Ti}$ static NMR spectra of (a) the as-made TiO_2 particles and after calcination at (b) 400 °C, (c) 650 °C, (d) 700 °C, and (e) bulk polycrystalline anatase.

Bastow and Whitfield for a titania gel annealed at 500 °C.²² As the annealing temperature increases up to 700 °C, the singularities of this shape become clearer and the line approaches that of bulk crystalline anatase. Above 700 °C, a second, broader line shape appears that can be identified with rutile. This broader peak is the only one remaining at 850 °C, in good agreement with the XRD results.

Samples Annealed at $T \leq 700$ °C. The $^{47,49}\text{Ti}$ static NMR spectrum of a specimen of commercial crystalline anatase (Aldrich) is shown in Figure 4e and is the superposition of the line shapes from the ^{47}Ti and ^{49}Ti isotopes separated by the difference in their Larmor frequencies of $^{49}\nu - ^{47}\nu = 9076$ Hz at 14.06 T. The spectrum was then simulated, by using the same electric field gradient and asymmetry parameter (η) for each site so that C_Q was scaled by the ratio of the quadrupole moments $^{49}\text{Q}/^{47}\text{Q} = 0.8275$.¹⁸ The quadrupolar parameters obtained presented in Table 1 are in good agreement with those previously proposed.^{15,19,21,22} The isotropic chemical shift value of approximately -67 ppm is in good agreement with the value obtained in the MAS NMR study of Dec et al.²¹

Below 700 °C the spectra obtained for the TiO_2 nanoparticles could be well simulated (Figure 4) by using the same quadrupolar parameters but with additional Lorentzian apodization to smooth the line. The amount of Lorentzian smoothing decreases with increasing annealing temperature (Table 2). The corresponding sizes of the particles determined from the line width of the (101) diffraction peak of the X-ray patterns (Figure 2) are also given in Table 2. XRD indicates

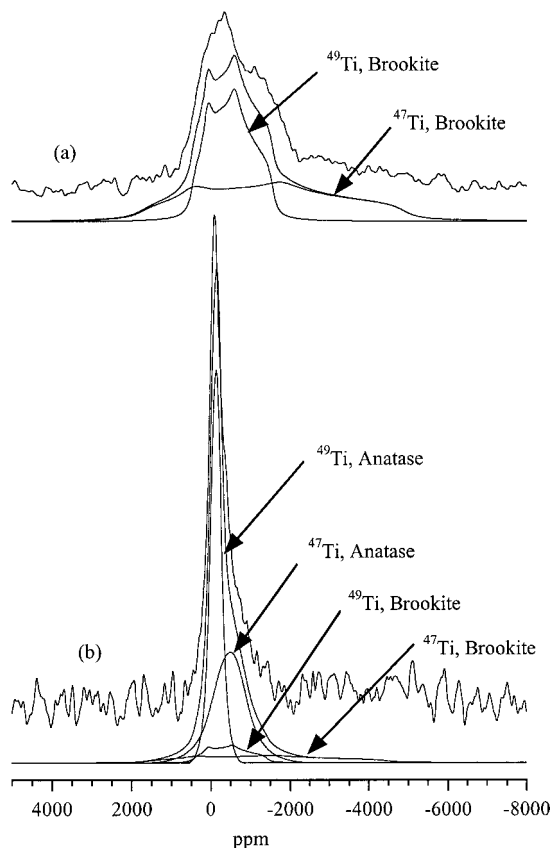


Figure 5. Experimental and simulated $^{47,49}\text{Ti}$ static NMR spectra of (a) TiO_2 crystalline brookite and (b) as-made particles.

Table 2. Dependence on the Annealing Temperature (T_p) of the Mean Particle Size Determined from XRD and Lorentzian Apodization Used in the $^{47,49}\text{Ti}$ NMR Spectral Simulations

T_p (°C)	400	550	650	700	
size (nm) (± 0.4)	5	7.5	11	17	19
apodization (kHz) (± 0.1)					
^{49}Ti	8.0	7.2	6.8	6.0	4.8
^{47}Ti	24.6	21.7	16.8	11.5	5.8

anatase structure in these nanoparticles below 700 °C. The degree of order increases with annealing temperature and the X-ray reflections narrow. The $^{47,49}\text{Ti}$ NMR spectra are also characteristic of anatase with the features of the second-order quadrupolar pattern sharpening so that less smoothing is required with increasing annealing temperature. This broadening is indicative of a spread of parameters resulting from a range of local environments that is greater in the less ordered materials.

The XRD patterns obtained for TiO_2 particles heat-treated up to 650 °C also show a small proportion of brookite, which is not obvious on the $^{47,49}\text{Ti}$ NMR spectra. The $^{47,49}\text{Ti}$ NMR spectrum of brookite crystallized under hydrothermal conditions²⁶ is presented in Figure 5a. The resonance is much broader than that from anatase and could be simulated with C_Q approximately twice that of anatase (Table 1). The ^{49}Ti (1/2, -1/2) transition lies on top of the much broader one for ^{47}Ti . The value of η is consistent with that in ref 12 but the values of C_Q and the isotropic chemical shift do not agree between the two studies. However,

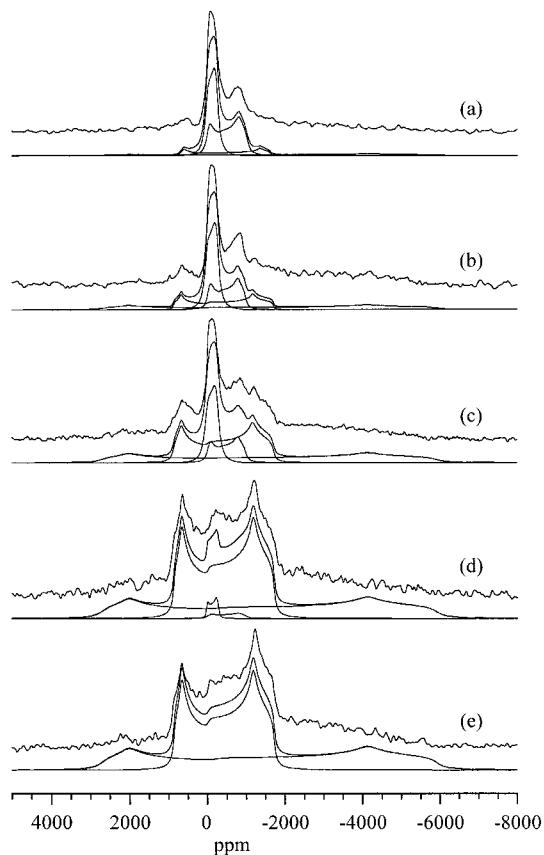


Figure 6. Experimental and simulated $^{47,49}\text{Ti}$ static NMR spectra of the TiO_2 particles annealed at (a) 700 °C, (b) 730 °C, (c) 770 °C, (d) 800 °C, and (e) 850 °C.

as was noted in ref 12, large differences appear in the titanium NMR spectra from different brookite samples.

With the parameters for brookite obtained here, the spectrum of the as-made nanoparticles was simulated using both anatase and brookite components in the proportion (80/20) obtained from the X-ray diffraction patterns (Figure 5b). This ratio is reflected in the NMR spectra by the integrated intensity of the ^{49}Ti features from the two phases. The resulting shape is not very different from the pure anatase because the brookite line shape is much broader and is of relatively low integrated intensity. Hence, although it is possible to simulate the $^{47,49}\text{Ti}$ NMR spectra from such samples, it would not be possible to unambiguously identify the presence of the relatively small amounts of brookite in these samples on the basis of the NMR spectra alone.

Samples Annealed at $T \geq 700$ °C. Between 700 and 800 °C, the coexistence of TiO_2 anatase and rutile in various proportions is expected from the XRD patterns (Figure 2). The $^{47,49}\text{Ti}$ static NMR spectrum of the particles heat-treated at 770 °C shows quite clearly, in addition to the anatase shape, the presence of discontinuities that can be identified by their positions as being from rutile (Figure 6c). The $^{47,49}\text{Ti}$ NMR static spectrum of rutile (Figure 6e) has a much broader frequency spread than anatase. Hence, only the ^{49}Ti NMR spectrum is efficiently excited and the edges of the ^{47}Ti resonance are not clearly observed. The ^{49}Ti centerband shape could be fitted with quadrupolar parameters (Table 1) in good agreement with those already reported^{15,21} and the isotropic chemical shift is also in broad agreement.¹⁵

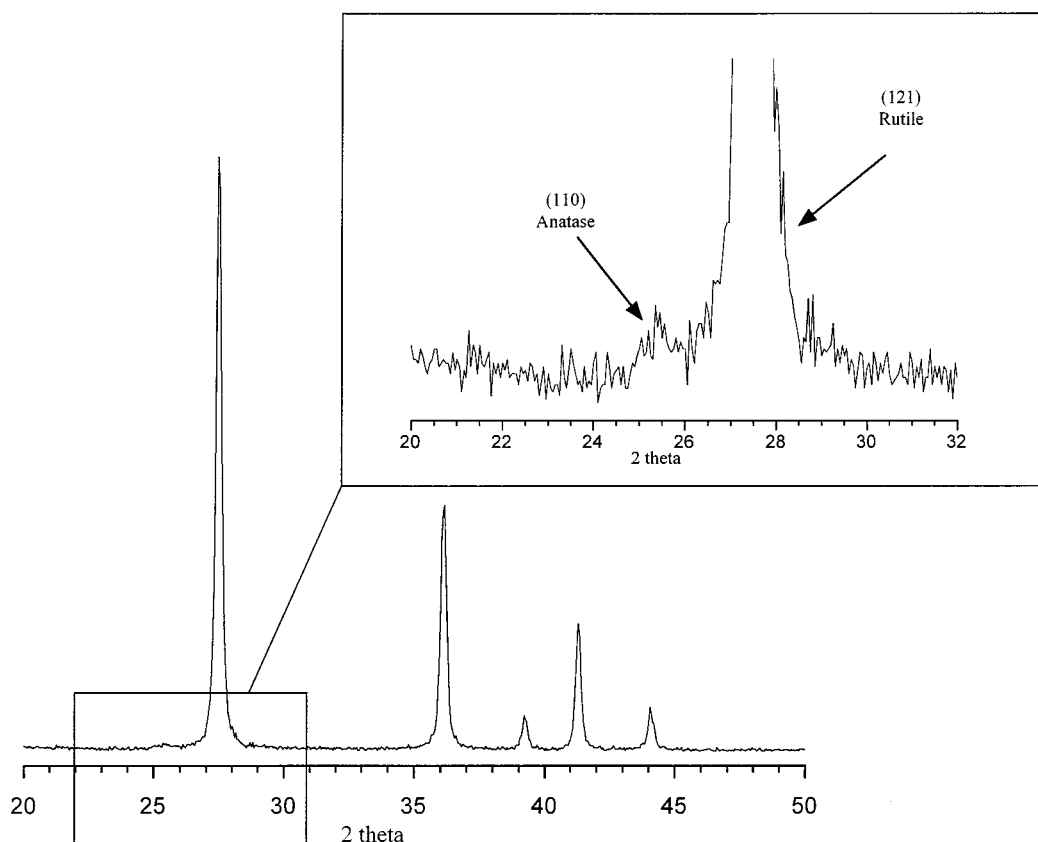


Figure 7. XRD patterns of the TiO_2 particles annealed at 800 °C together with an expansion of the 2θ range between 20° and 32°.

Table 3. Percentages of Anatase and Rutile in Titania Nanoparticles Heat-Treated at Temperatures (T_p) $T \geq 700$ °C, Extracted from XRD and ^{49}Ti NMR Spectral Simulations

T_p (°C)	% from XRD (± 2)		% from ^{49}Ti NMR (± 2)	
	anatase	rutile	anatase	rutile
700	72	28	70	30
730	60	40	58	32
770	28	72	26	74
800	2	98	4	96
850	0	100	0	100

Spectra of titania particles heat-treated above 700 °C were then simulated using both anatase and rutile shapes in different proportions (Figure 6). The resulting ratio between the two phases was extracted from these simulations by integration of the corresponding ^{49}Ti signals of the two phases (Table 3). The proportions of these phases were also calculated from the X-ray patterns by considering the ratio of the areas of the 110 and 121 diffraction peaks of the anatase and rutile phases, respectively. A calibration curve established by recording the XRD patterns of known mixtures of anatase and rutile¹⁴ was then used to deduce the true ratio of the two phases (Table 3). These calculations were made assuming that, according to the width of the diffraction lines, the domain sizes of the two phases were not very different. The results obtained by NMR and XRD are in excellent agreement and are complementary. For example, the amount of the rutile cannot

accurately be determined from the NMR spectrum of the 700 °C sample because of the low intensity of the broad rutile resonance, which is largely lost in the baseline (Figure 6a). However, the small amount of anatase in the 800 °C sample is quite difficult to evaluate from XRD (Figure 7). This small component can be easily observed and the amount determined from the NMR spectrum because the small but much narrower anatase signal is apparent on top of the broad rutile line shape (Figure 6d).

This study has clearly shown the utility of high-field solid-state titanium NMR for materials characterization. NMR is complementary to XRD and in TiO_2 nanoparticles the phase mixture of anatase and rutile can be quantified. With ever higher applied magnetic fields becoming available, this should encourage even wider application of titanium NMR in solids.

Acknowledgment. M.E.S. thanks the EPSRC for funding NMR equipment at Warwick and work on solid-state NMR characterization of gel-formed materials through GR/N64267. The collaboration between the laboratories in Warwick and Paris was funded through a CNRS/Royal Society grant. C.G. thanks the EU for a Framework V Marie Curie fellowship. The authors are grateful to Dr. Dominique Massiot (CNRS, Orléans) for his help in simulations of the spectra.

CM0011918